Fundamental Studies on Coulopotentiography

AUTHOR(S):

Yamada, Takeshi; Okazaki, Satoshi; Fujinaga, Taitiro

Bull. Inst. Chem. Res., Kyoto Univ., Vol. 56, No. 4, 1978

Fundamental Studies on Coulopotentiography

Takeshi YAMADA†, Satoshi OKAZAKI, and Taitiro FUJINAGA*

Received March 6, 1978

A new electroanalytical methodology has been proposed on the basis of flow-coulometry with controlled potential scanning, in which the total current, *i.e.* number of coulombs, is recorded against the applied potential.

The method not only has a great advantage of an absolute determination but also a great convenience for the continuous and simultaneous analysis of trace metal ions. Metal ions of a concentration higher than 10^{-6} *mol/l* were directly determined without preparing standards, and trace metal ions down to 10^{-8} *mol/l* were also determined by an anodic stripping coulopotentiography.

The proposed method has many methodological possibilities in analytical chemistry and also electrochemistry.

INTRODUCTION

It goes without saying that voltammetric methods have played an important part in analytical applications and also in studies of the mechanism of electrode reactions. In most of these methods, however, electrolysis is performed partly within the solution at the vicinity of the electrode surface called, the "diffusion layer." Quantitative analysis is carried out utilizing the fact that the diffusion current is proportional to the concentration of a depolarizer, so that the shape of the electrode and the factors which affect the process of mass transfer have delicate effects on the measurements. As a result, absolute determination based on the theoretical equation is exceedingly difficult.

In the coulometric method, as opposed to voltammetry, the objective depolarizers in the electrolysis solution are completely electrolyzed, and the determination is performed on the basis of Faraday's law. Thus, the coulometric method is said to be superior in the following points: (1) The quantities of electricity consumed in the electrolysis are measured regardless of the shape of the electrode or the rate of mass transfer in the electrode process; and (2) The amounts of depolarizers are absolutely determined without preparing any standard. On the other hand, conventional coulometry generally has such disadvantages as, insufficient sensitivity, relatively long electrolysis time, and difficulty in the simultaneous determination of the multi-components system.

Recent development in coulometry has overcome these disadvantages one after the other. For instance, from the standpoint of rapid electrolysis, many attempts at improving the coulometric cell have been made by Eckefeldt,[1] Fujinaga,[2~4] Blaedel,[5] Bard,[6] Johanson,[7] Muto[8] and others.[9,10] Fujinaga and his collaborators[11,12]

* 山田　武，岡崎　敏，藤永太一郎：Department of Chemistry, Faculty of Science, Kyoto University, Sakyo-ku, Kyoto 606 Japan.

† Present address: Faculty of Textile Science, Kyoto Technical University, Sakyo-ku, Kyoto 606 Japan

developed a chromatographic method of electrolytic analysis with a column electrode of continuous potential gradient for the consecutive determination of metals. In addition, Propst[13] developed a method for simultaneous determination in batchwise coulometry by recording analog-integrated coulograms.

The authors[14,15] have developed a new electroanalytical methodology called "Coulopotentiography." It is based on flow-coulometry with controlled potential scanning in which the total current, *i.e.* the number of coulombs, is recorded against the applied potential. The half-wave potenital of a coulopotentiogram offers qualitative authority, and also the limiting current gives a quantitative ground for the concentration of a depolarizer as conveniently as in polarography. The method gives more precise qualitative and quantitative data than the conventional flow–coulometry at constant potential

Metal ions of a concentration higher than 10^{-6} *mol/l* were directly analyzed without preparing a standard, and trace metal ions of a concentration down to 10^{-8} *mol/l* were also determined by combining them using an anodic stripping technique, *i.e.* anodic stripping coulopotentiography.

The method is also useful for the study of the mechanism of electrode reaction.

FUNDAMENTALS

Rapidity and Sensitivity of the Electrolysis with the Column Electrode

Controlled potential electrolysis usually proceeds according to the following equation,[16]

$$i_t = i_0 \exp[-\lambda t] \qquad \cdots\cdots\cdots(1)$$

where, i_0 is the initial current, i_t is a current at time t and λ is the cell factor (sec^{-1}) which depends on experimental conditions such as electrode dimension, solution volume, cell geometry and rate of mass transfer. The amount of electricity Q (coulombs) consumed in the electrolysis is given by Eqs. (2) and (3),

$$Q = \int_0^\infty i_0 \exp[-\lambda t]\, dt \qquad \cdots\cdots\cdots(2)$$

$$i_0 = 2.303\lambda \cdot Q \qquad \cdots\cdots\cdots(3)$$

Equation (3) suggests that the larger the cell factor, the higher the sensitivity that is expected for a given Q. In conventional electrolysis, the λ value can hardly exceed 0.005 sec^{-1}. The λ value of the column electrode used in this study was so large, of the order of 1 sec^{-1}, that the electrolysis was completed within ten seconds. Moreover, the limiting current of the order of microamperes was expected for the electrolysis of one coulomb which corresponds to minute amounts of the depolarizer of 10^{-11} equiv.

Equation of the Limiting Current

In coulopotentiography with a column electrode, the assumption that the objective depolarizer flew into the column will immediately attain equilibrium with the electrode is virtually satisfied. The following equation is derived from Faraday's law,

$$Q = F \cdot W = F \cdot n \cdot C \cdot V \qquad \cdots\cdots(4)$$

where, F is the Faraday constant (96500 C per equiv.), W is the number of the chemical equivalent, n is the number of electrons gained or lost per molecule in the electrode reaction, C is the concentration (*mol/l*) of a depolarizer, and V is the volume (*l*) of the electrolysis solution. The limiting current i_l (amperes) is expressed by Eq. (5),[17]

$$i_l \equiv \frac{dQ}{dt} = 96500\, n \cdot C \cdot \frac{dV}{dt} = 96500\, n \cdot C \cdot f \qquad \cdots\cdots(5)$$

in which f is the volume flow rate (*l*/sec). Thus the concentration of the depolarizer can be directly calculated from the observed values of the limiting current and the flow rate by Eq. (5).

Characteristics of Coulopotentiogram for a Reversible Redox System

When Oxidant and Reductant are Both Soluble in the Solution:

As the column electrode is compactly packed with fine grains of glassy carbon, and the surface area of the electrode is extremely large relative to the cell volume, the solution layer surrounding the electrode surface may be as thin as that in the thin layer electrode. When the reversible electrode reaction takes place between the soluble oxident Ox and the soluble reductant Red, and obeys the Nernst equation, a simple approach is given below.

$$Ox + ne \rightleftharpoons Red \qquad \cdots\cdots(6)$$

The concentration of Ox and Red can be assumed to be uniform throughout the cavity as in a thin layer electrode. The total quantity of reactant present in the cavity is constant. If the initial concentration of reduced species is zero,

$$C_{Ox}^{I} = C_{Ox} + C_{Red} \qquad \cdots\cdots(7)$$

where C_{Ox}^{I} is the initial concentration of oxidant. Combining this with the Nernst equation yields an expression for the current-potential curve as follows,

$$i = n \cdot F \cdot f \cdot C_{Ox}^{I} \left\{ 1 + \exp\left[\frac{nF}{RT} (E - E^0) \right] \right\}^{-1} \qquad \cdots\cdots(8)$$

Thus the coulopotentiogram for the reversible redox couple in which both members are soluble in the solution shows a S-shaped curve similar to the polarogram. The electrolysis current reaches the limiting value when the electrode potential becomes sufficiently negative.

$$i_l = n \cdot F \cdot f \cdot C_{Ox}^{I} \qquad \cdots\cdots(9)$$

The combination of Eq. (8) with Eq. (9) yields the following practical equation at 25°C.

$$E = E_{1/2} + \frac{0.059}{n} \log\left[\frac{i_l - i}{i} \right] \qquad \cdots\cdots(10)$$

For Metal Deposition:

In the case of the reversible electro-deposition of a metal which sufficiently covers the electrode surface, the Nernst equation, Eq. (12), is applied.

$$M^{n+} + ne^- \rightleftharpoons M^0 \qquad \cdots\cdots(11)$$

$$E = E^0 + \frac{RT}{nF} \ln C_{M^{n+}} \qquad \cdots\cdots(12)$$

where, $C_{M^{n+}}$ is the concentration of the metal ion. The initial concentration of the metal ion $C^I_{M^{n+}}$ is expressed by Eq. (13).

$$C^I_{M^{n+}} = C_{M^{n+}} + \frac{i}{n \cdot F \cdot f} \qquad \cdots\cdots(13)$$

Combining Eq. (12) with Eq. (13) yields an expression for the coulopotentiogram of metal deposition.

$$i = n \cdot F \cdot f \cdot \left\{ C^I_{M^{n+}} - \exp\left[\frac{nF}{RT} (E - E^\circ) \right] \right\} \qquad \cdots\cdots(14)$$

Thus the current-potential curve for metal deposition shows a steep special pattern at the beginning and has no inflection point. The current also reaches the limiting value at a sufficiently negative potential.

$$i_l = n \cdot F \cdot f \cdot C^I_{M^{n+}} \qquad \cdots\cdots(15)$$

The combination of Eq. (14) with Eq. (15) yields the practical equation, Eq. (16) at 25°C.

$$E = E^\circ + \frac{0.059}{n} \log [i_l - i] \qquad \cdots\cdots(16)$$

Equation (17) indicates the positive shift of the half-wave potential with increasing concentration of metal ions.

$$E_{1/2} = E^{\circ\prime} + \frac{0.059}{n} \log [i_l/2] \qquad \cdots\cdots(17)$$

REAGENTS AND INSTRUMENTS

Reagents

All the chemicals used were of analytical reagent grade. Deionized water was used after being distilled from an all-quartz ware. Acidic potassium chloride supporting electrolyte solution was prepared by dissolving 1 *mole* of KCl and 0.1 *mole* of acetic acid into a 1 *l* volumetric flask. Acidic potassium chloride-potassium iodide carrier solution was also prepared by dissolving 1.0 *mole* of KCl, 0.01 *mole* of KI and 0.1 *mole* of acetic acid into a 1 *l* volumetric flask.

Column Electrode

Figure 1 shows a vertical sectional view of the column electrode made by Shibata

Chemical Instrument Co. Ltd. Glassy carbon grains from 80 to 100 mesh (Tokai Denkyoku Mfg. Co., GC-20) were packed tightly in a porous glass tube of 6.5 mm in diameter and 20 mm in length. A silver plate counter electrode and a silver-silver chloride reference electrode (SSE) were used.

Silver-Silver Chloride Reference Electrode

A silver wire (99.99 %) polished with fine emery paper was made so as to have small double rings at one end. These rings were burned by a gas burner to remove the organic compounds. Then the rings were dipped into fused silver chloride to form the thin film of silver chloride surrounding them. The electrode was inserted into the reference electrode vessel filled with saturated potassium chloride and silver

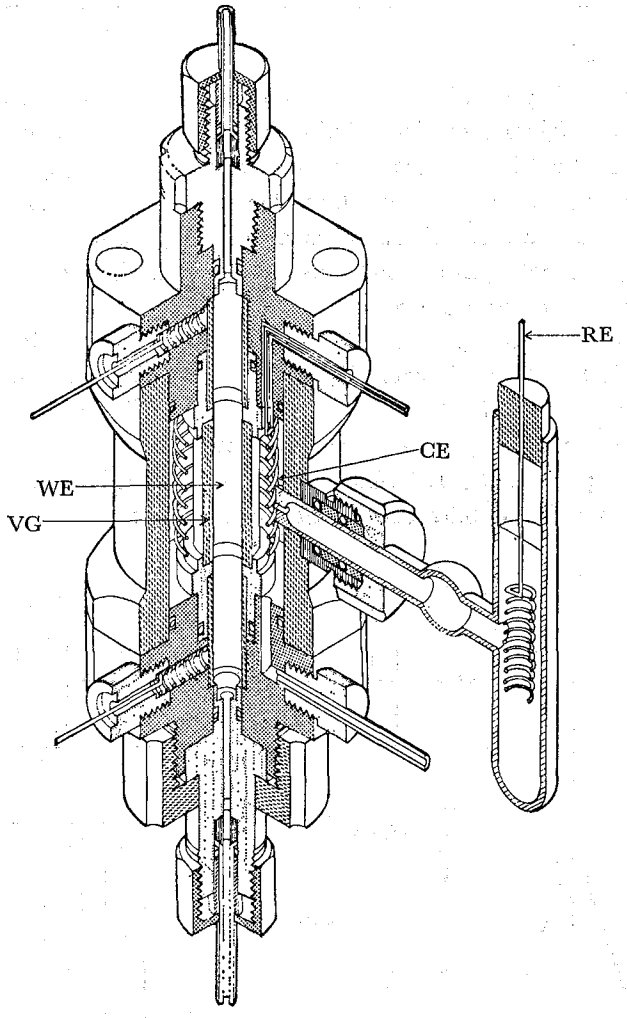

Fig. 1. Vertical sectional view of the column electrode.
WE: working electrode, RE: reference electrode,
CE: counter electrode, VG: vycor glass tube.

chloride solution. This electrode showed a very stable potential and had a very long life.

Apparatus

A Shibata potentiostat was used for coulometric detection and a self-made one for potential scanning coulometry.

A mechanical potential scanner was made by this laboratory. It was composed of a Beckman ten-turn potentiometer (10 Kohm), a synchronous motor (Japan Servo, 1800 r.p.m.) and a gear unit moderator. Ten ranges in scanning time and four ranges in span voltage were selectable.

A Shibata constant volume pump SP-200 (200 *ml/hr* max.) with a difron head was used.

Use was also made of a National 2-pens recorder VP-654A with a current adapter.

Instrument and Procedure

A Schematic diagram of the single cell coulopotentiograph is shown in Fig. 2. Acidic potassium chloride carrier solution containing copper, lead and cadmium ions, each of 10^{-4} *mol/l* after deoxygenated by bubbling nitrogen gas, was passed through the cell at a constant flow rate of 2 *ml*/min with a constant volume pump. After the potentiostat was set with such conditions as the initial potential, scan range and scan rate, the potential scanner was started, and the electrolysis current was recorded against the electrode potential.

A typical coulopotentiograms of copper, lead and cadmium in acidic potassium chloride base electrolyte are shown in Fig. 3. Four waves correspond to the electrode reaction of Cu^{2+} to Cu^{+}, Cu^{+} to Cu^{0}, Pb^{2+} to Pb^{0} and Cd^{2+} to Cd^{0}, respectively. The concentration of lead ions, for instance, was calculated from the observed data; $i_l = 6.4 \times 10^{-4}$ amp., $f = 3.33 \times 10^{-5}$ *l*/sec, and Eq. (5). Good accordance between the observed concentration of 9.97×10^{-5} *mol/l* and the taken concentration of 1.0×10^{-4}

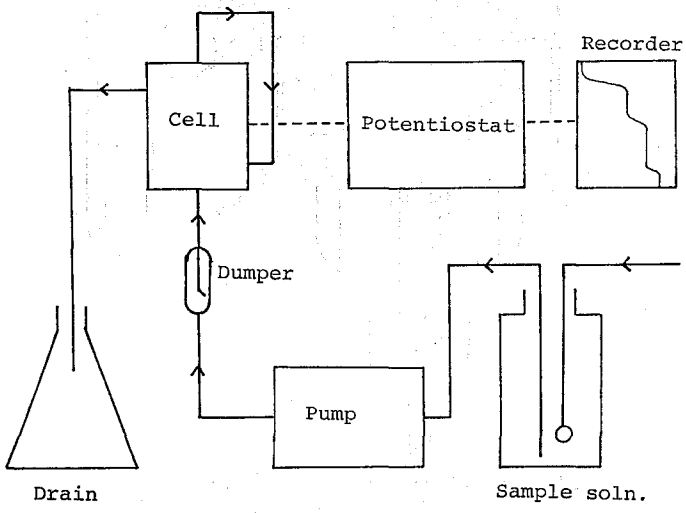

Fig. 2. Schematic diagram of a single cell coulopotentiograph.

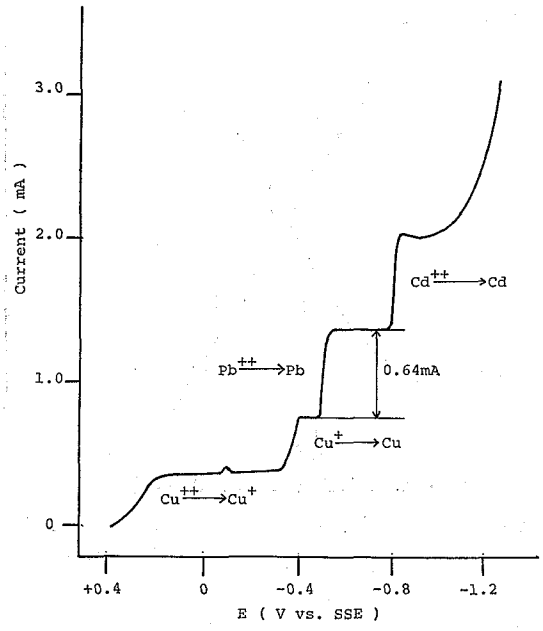

Fig. 3. Coulopotentiogram of Cu^{2+}, Pb^{2+}, and Cd^{2+}. Sample: $10^{-4}M$ Cu^{2+}, Pb^{2+}, and Cd^{2+} in $0.1M$ $CH_3COOH+1M$ KCl, flow rate: 2 *ml*/min, scan rate: 36 mV/min.

mol/*l* was obtained.

RESULTS AND DISCUSSION

Coulopotentiography of Ferricyanide Ions

Figure 4 shows the coulopotentiograms of $10^{-4}M$ $Fe(CN)_6^{3+}$ in $1M$ KCl. Curve 1 illustrates i-E curve obtained with a slow scan rate of 2.67 mV/min, and line 3 is a log-plot line according to Eq. (10). The observed slope of 60 mV agreed with the theoretical value of 59.1 mV for one electron reversible reduction. Curve 2 demonstrates the one obtained with a rapid scan rate of 26.7 mV/min. No notable effect of the scan rate on the electrode reaction was observed between curves 1 and 2.

Figure 5 shows the effect of the concentration of a depolarizer upon the i-E curves. The shape of the current-potential curve tended to be distorted with increasing concentration. Figure 6 indicates the relationship between the half-wave potential and the current at the half-wave potential. The linear relationship suggested that the distortion of the wave at the higher concentration region was due to ohmic potential drop. The slope gave the internal resistance of the column electrode and was 11.3 ohms.

The internal resistance of the cell was also calculated from Eq. (18)

$$E = E_{1/2}+\frac{0.059}{n}\log\left[\frac{i_l-i}{i}\right]+iR \qquad \cdots\cdots\cdots(18)$$

where, R is the internal resistance of the cell. A FORTARN program for the wave

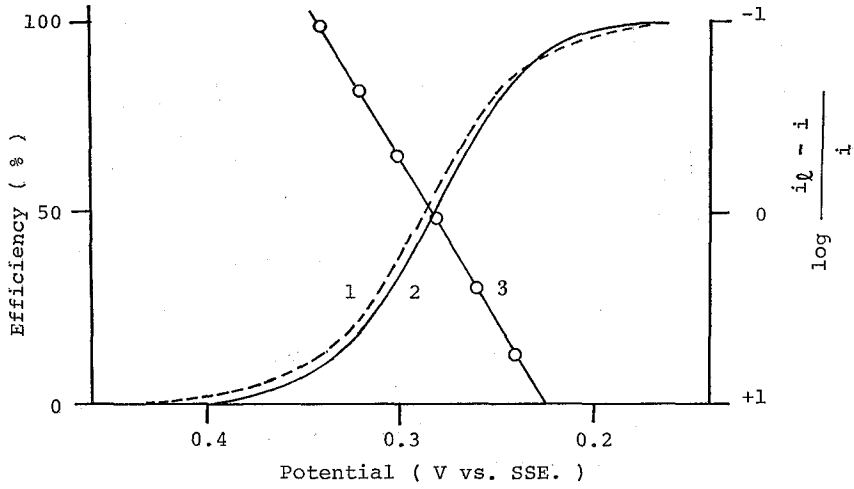

Fig. 4. Coulopotentiogram of ferricyanide ions and wave analysis. Sample: $10^{-4}M$ $Fe(CN)_6^{3-}$ in 1 M KCl, flow rate: 2 *ml*/min, scan rate: 1) 2.67 mV/min, 2) 26.7 mV/min, 3) 2.67 mV/min.

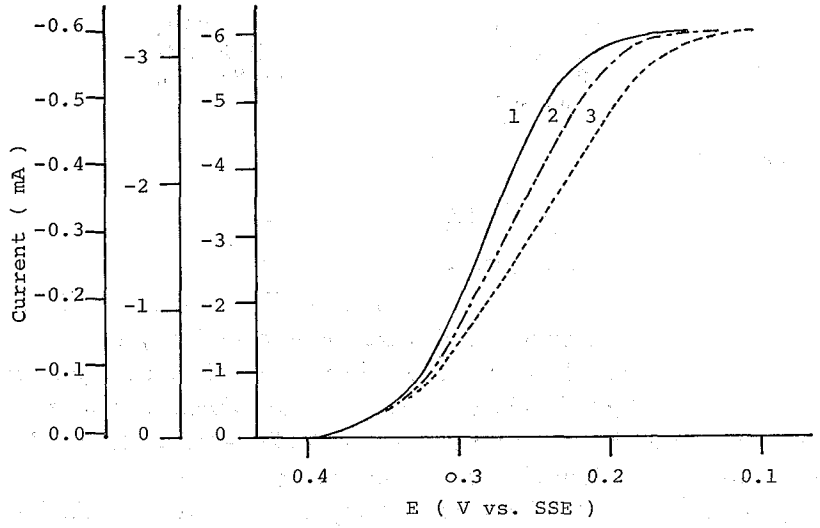

Fig. 5. Effect of the concentration on the coulopotentiogram of ferricyanide ions. Concentration of $Fe(CN)_6^{3-}$: 1) $10^{-4}M$, 2) $10^{-3}M$, 3) $2\times10^{-3}M$ Carrier solution: 1M KCl, flow rate: 2 *ml*/min, scan rate: 2.67 mV/min

analysis using the non-linear least square method was written to give the cell resistance, half-wave potential, limiting current, log-plot slope, and intercept of base current. The cell resistance calculated by this method was 11.1 ohms, and very good agreement was obtained between the graphical and the computer method. The FACOM 230–75 computer at Kyoto University's Data Processing Center was used, and the calculation time was only 0.13 sec per wave.

As the coulopotentiography generally deals with relatively large current, the cell resistance is one of the most important problems. The cell resistance changes due

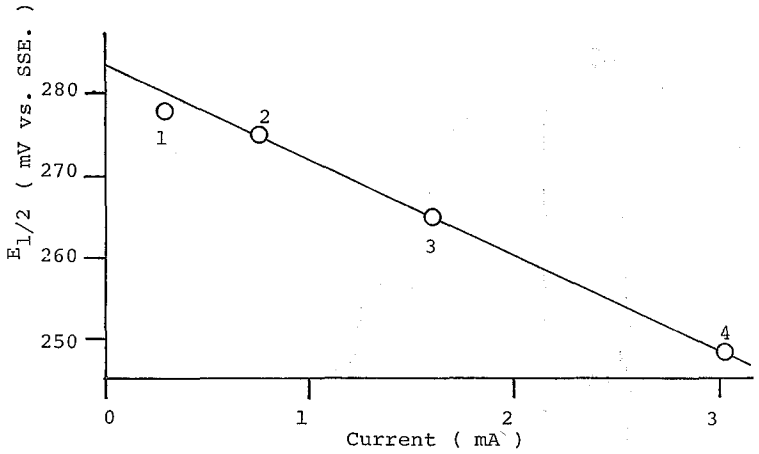

Fig. 6. Relation between $E_{1/2}$ and $I_{E_{1/2}}$.
Sample: $Fe(CN)_6^{3-}$ in 1 *M* KCl, flow rate: 2 *ml*/min, scan rate: 2.67 mV/min, Concentration: 1) 2×10^{-4} *M*, 2) 5×10^{-4} *M*, 3) 10^{-3} *M*, 4) 2×10^{-3} *M*

to the condition of packing of glassy carbon grains. Recently, a smaller resistance cell of 3.2 ohm was used.

Coulopotentiography of Metal Ions

Coulopotentiograms of lead ions in acidic KCl based solution are shown in Fig. 7. The waves showed asymmetric S-shaped curves. Discordance of wave shapes between observed and theoretical ones seemed to be due to insufficient surface coverage of deposited lead. As a result, this tendency became more significant with decreasing concentration of lead ions.

The result of wave analysis according to Eq. (16) is shown in Fig. 8. The

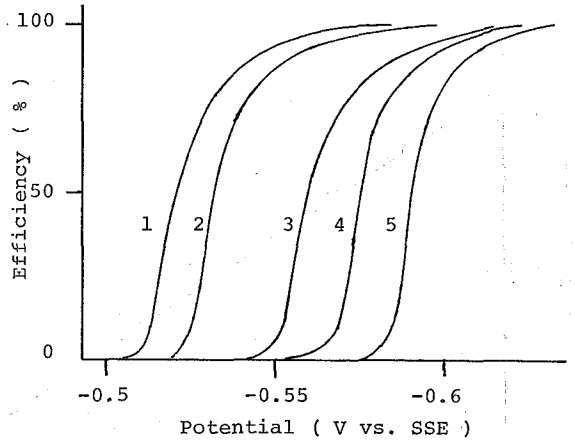

Fig. 7. Influence of concentration on the couloptentiogram of lead ions.
Concentration: 1) 10^{-4} *M*, 2) 5×10^{-5} *M*, 3) 10^{-5} *M*, 4) 5×10^{-6} *M*, 5) 2×10^{-6} *M*, carrier solution: 0.1 *M* CH_3COOH+1 *M* KCl, flow rate: 2 *ml*/min, scan rate: 1.33 mV/min.

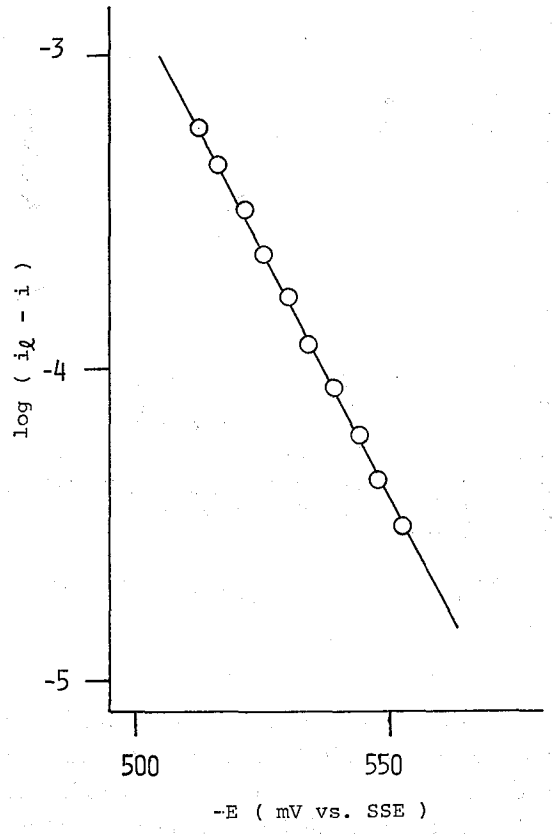

Fig. 8. Wave analysis for Pb^{2+} wave.
Sample: 10^{-4} *M* Pb^{2+} in 0.1 *M* CH_3COOH+1 *M* KCl, flow rate: 2 *ml*/min, scan rate: 1.33 mv/min.

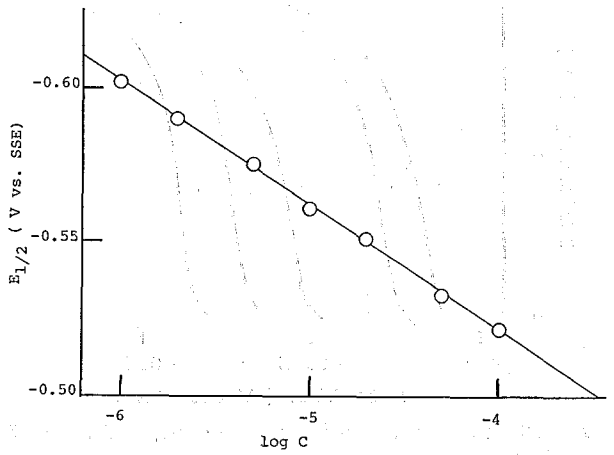

Fig. 9. Dependence of $E_{1/2}$ of Pb^{2+} on the concentration.
Carrier solution: 0.1 *M* CH_3COOH+1*M* KCl, flow rate: 2 *ml*/min, scan rate: 1.33 mV/min.

log-plot slope of 28 mV indicates reversible two electron reduction. The half-wave potentials moved to a more positive direction with increasing concentration of lead ions as shown in Fig. 9.

Figure 10 shows a comparison of the coulopotentiogram (curve A) in 1*M* HCl with the coulomb-potential curve (curve B) obtained by conventional flow-coulometry at constant potential. The ratios of the wave height of the first cupric wave to that of the second cuprous wave in the conventional coulomb-potential curve and in the coulopotentiogram were 6:4 and 5:5, respectively. In the conventional method, it was considerably more difficult to obtain a good reproducibility because of the difficulty of maintaining the surface conditions of the column electrode unchanged and also due to concentration non-uniformity of a depolarizer injected into the column electrode.

It may be concluded that the method gave more precise qualitative and quantitative data than the conventional flow-coulometry at constant potential.

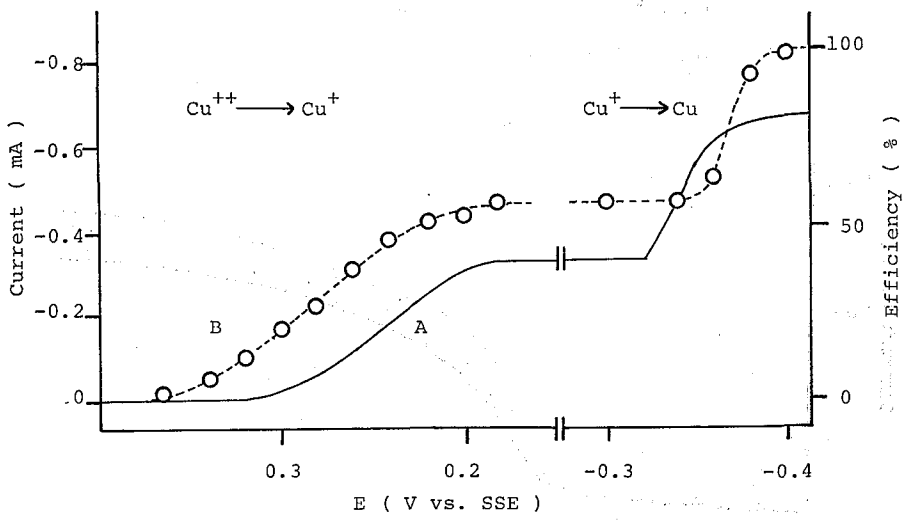

Fig. 10. Coulopotentiogram (A) and coulogram (B) of Cu^{2+}.
Sample: 10^{-4} *M* Cu^{2+} in 1 *M* HCl, flow rate: 2 *ml*/min, scan rate: 1.33 mV/min, sample size in the conventional method: 50 μl of 10^{-2} *M* Cu^{2+}.

Determination of Lead and Ferricyanide Ions

The concentration of the depolarizer can be absolutely determined from the experimental data of limiting current and flow rate using Eq. (5). Acidic KCl carrier solution is recommended for the determination of lead ions due to the small base current. The analytical result for the standard sample of lead ions is summarized in Table I. The average recovery for 10^{-5} *M* Pb^{2+} is 100.5 % with a relative standard deviation of 1.6 %. This method has a wide application range of concentration.

Figure 11 shows the coulopotentiogram of very dilute lead ions of 1×10^{-6} *mol*/*l*. The effect of the residual current became remarkably large at low concentration,

Table I. Determination of Pb^{2+} Standard Sample

Carrier soln: 1*M* KCl+0.1*M* CH_3COOH, flow rate: 2 ml/min, scanning rate: 1.33 mV/min.

Concentration (*mol/l*)	Electrolysis efficiency (%)	σ* (%)
1×10^{-3}	97.9	
5×10^{-4}	96.7	
2×10^{-4}	96.5	
1×10^{-4}	103.0	
5×10^{-5}	97.5	
2×10^{-5}	98.0	
1×10^{-5}	100.5	1.6
5×10^{-6}	106.0	
2×10^{-6}	105.1	
1×10^{-6}	115.9	

* Relative standard deviation

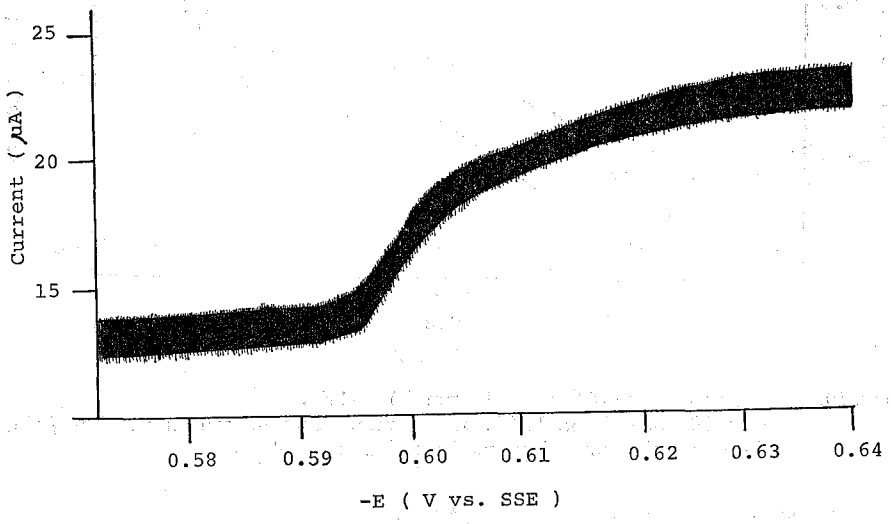

Fig. 11. Coulopotentiogram of very dilute lead ions.
Sample: 10^{-6} *M* Pb^{2+} in 0.1 *M* CH_3COOH+1 *M* KCl, flow rate: 2 *ml*/min, scan rate: 1.33 mV/min.

less than 10^{-6} *mol/l*, and the accuracy in the quantitative analysis fell to some extent.

Table II summarizes the result of the determination for ferricyanide ions in 1*M* KCl carrier solution. The determination limit for ferricyanide ion was somewhat high in comparison with that for lead ion because of a relatively large base current of 1*M* KCl base solution.

Table II. Determination of $Fe(CN)_6^{3-}$ Standard Sample

Carrier soln: 1*M* KCl, flow rate : 2 ml/min, scanning rate: 1.33 mV/min.

Concentration (*mol/l*)	Electrolysis efficiency (%)	σ* (%)
1×10^{-3}	97.4	0.7
5×10^{-4}	97.2	0.8
2×10^{-4}	97.5	2.3
1×10^{-4}	97.6	2.3
5×10^{-5}	97.4	1.9
2×10^{-5}	100.3	0.8
1×10^{-5}	88.4	

* Relative standard deviation

Double Cell Coulopotentiography

In a way similar to that used in voltammetry, it is found that the effect of the charging current becomes serious at a high scan rate or for very dilute samples. In this method, however, this kind of trouble could easily be overcome by using the double cell method mentioned below.

As shown in Fig. 12, two column electrodes are closely connected but controlled independently by two potentiostats. The electrode potential of the first cell was scanned linearly, but that of the seconed cell was kept constant to detect depolarizers passed through the first cell. The current-potential curve is obtained by plotting the electrolysis current through the second cell against the electrode potential of the first cell. Thus the effect of the charging current caused by potential scanning was successfully eliminated. The influence of the potential scan-rate upon the electrolysis efficiency of ferricyanide ion is summarized in Table III.

The scanning rate in the range from 1.3 mV/min to 180 mV/min had no effect on either the current efficiency or the shape of the current-potential curve. A linear shift of the half-wave potential with increasing scanning rate was observed as shown in Fig. 13. In the figure, line A indicates the negative shift of the half-wave potential measured by negative scanning from +0.5 V *vs.* SSE, and line B shows the positive shift in positive scanning from +0.1 V *vs.* SSE, while dotted line indicates the constancy of the average half-wave potential. The effluent from the first cell was detected by the second cell at a constant potential of 0 V *vs.* SSE. Wave analysis of these current–potential curves suggested a reversible electrode process even at a high scanning rate of 180 mV/min. From these facts, shift of the half-wave potential of the double cell method seemed to be due to the dead volume between the two cells. The usable high scanning rate is restricted by the response time of the column electrode, *i.e.* the λ value of the column electrode.

The double cell method is useful not only for shortening of the analysis time but also for expanding of the determination limit of a more dilute concentration by combining with the anodic stripping technique, as mentioned below.

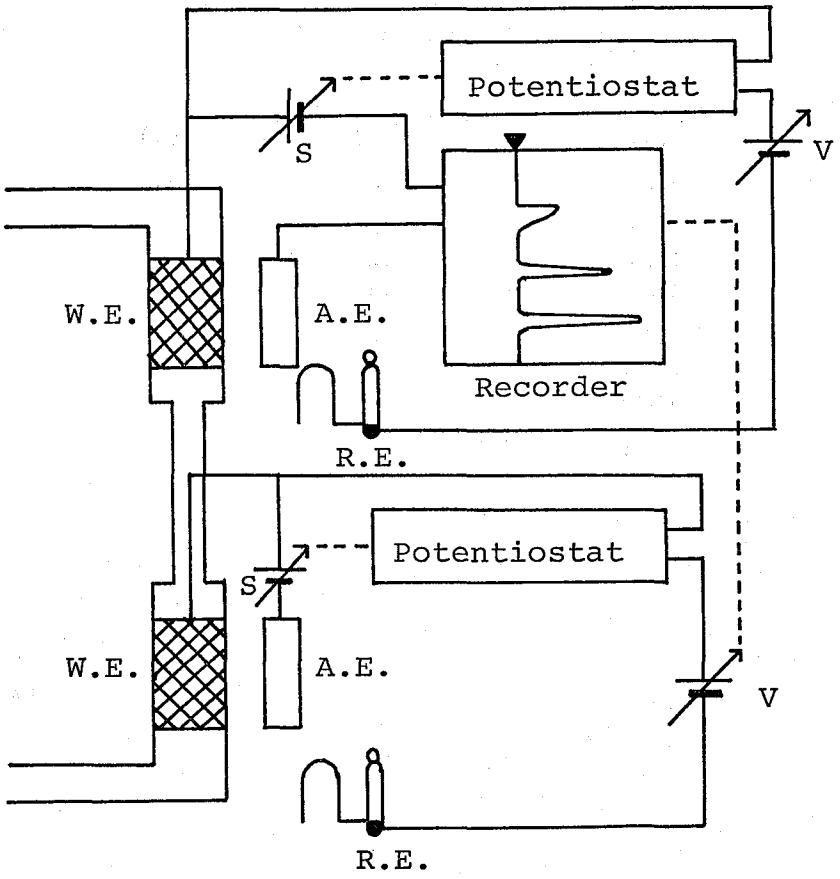

Fig. 12. Schematic diagram of a double cell coulopotentiograph.
WE: working electrode, RE: reference electrode, AE: counter electrode, S: electric source, V: applied voltage.

Table III. Effect of Scan Rate on Electrolysis Efficiency

Sample : 10^{-4} *mol/l* $K_3Fe(CN)_6$, carrier soln: 1*M* KCl, flow rate: 2 *ml*/min.

Scanning rate (mV/min)	Electrolysis efficiency (%)
1.33	100.1
2.67	103.8
5.33	100.0
8.00	98.0
16.0	101.3
26.7	98.7
40.0	99.3
90.0	98.2
180.0	97.8
360.0	97.3

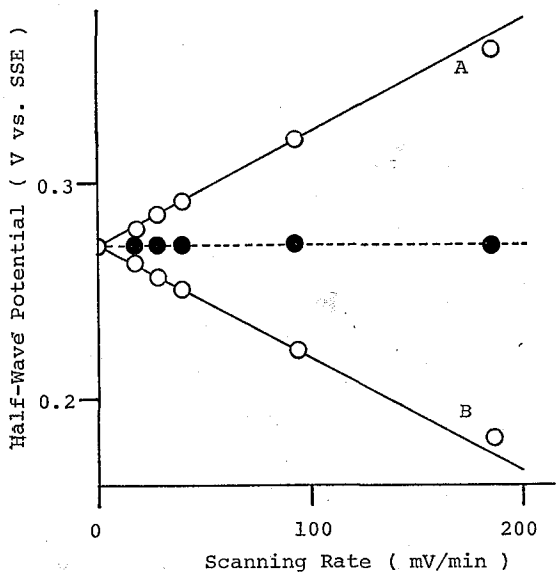

Fig. 13. Influence of scan rate upon $E_{1/2}$ using the double-cell method. Sample: $10^{-4}M$ $Fe(CN)_6^{3-}$ in $1M$ KCl, flow rate: 2 *ml*/min, curve A: negative scan from +0.5 V *vs.* SSE, curve B: positive scan from +0.1 V *vs.* SSE.

Anodic Stripping Coulopotentiography

Though the method is sensitive enough for direct analysis, signal to noise ratios and the accuracy of the determination fall for the dilute sample below 10^{-6} *mol/l*. An improvement was carried out, however, by combination with an anodic stripping technique in the same manner as in voltammetry. Moreover, great enhancement of sensitivity was achieved by combining the stripping method with the double cell method.

Stripping Coulopotentiography with a Single Cell:

In this method, the initial potential of the column electrode was kept sufficiently negative to deposit all metal ions for a definite period. After that, the electrode potential was swept to the positive direction to dissolve the deposited metal. The stripping current was plotted against the scanning potential. The typical stripping curve of cadmium, lead and copper is shown in Fig. 14. These ions of 5×10^{-7} moles each were initially codeposited at -1.2 V *vs.* SSE, then deposited metals were dissolved in turn at the scan rate of 36 mV/min. Although this method is simple, very convenient and sensitive, the effect of the base current is remarkable. From the viewpoint of sensitivity, the double cell method may be superior.

Stripping Coulopotentiography with a Double Cell:

For the analysis of a very dilute solution, less than 10^{-7} *mol/l*, preliminary concentration is extremely effective. For this, another method utilizing anodic stripping with a double cell is recommended.

In Fig. 12, the first cell was used for pre-concentration and stripping, and

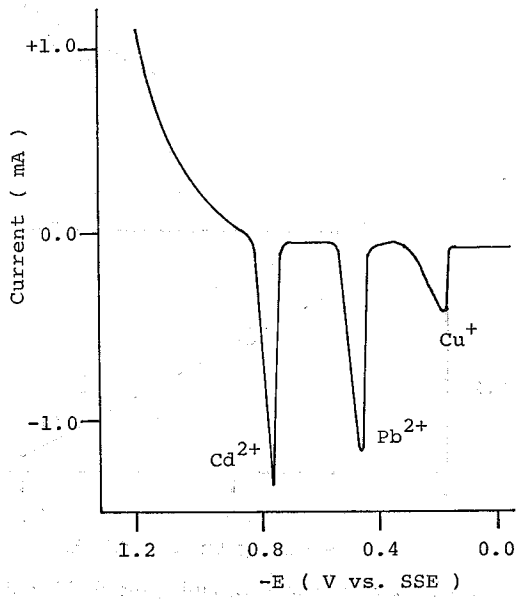

Fig. 14. Stripping coulopotentiogram of Cd^{+2}, Pb^{2+}, and Cu^{2+} with a single cell.
Sample: 5×10^{-7} *mole* each Cd^{2+}, Pb^{2+}, and Cu^{2+} in 0.1 *M* $CH_3COOH+1M$ KCl, flow rate: 2 *ml*/min, scan rate: 36 mV/min, deposition potential: −1.2 V *vs.* SSE.

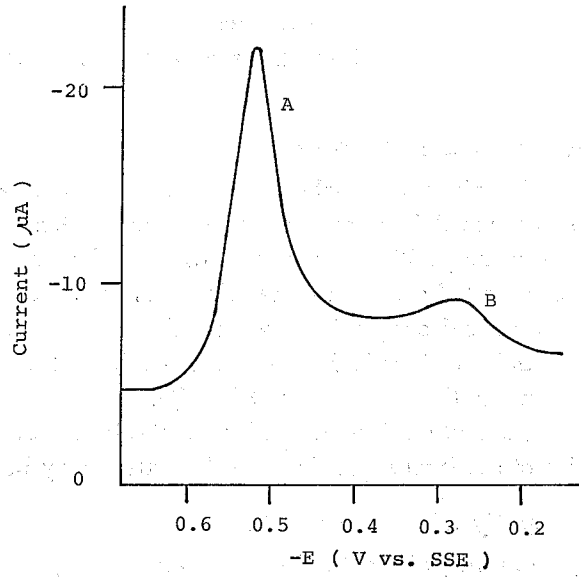

Fig. 15. Stripping curve of trace lead with double-cell.
Sample: 250 *ml* of 10^{-8} *M* Pb^{2+}, carrier solution: 0.1 *M* CH_3COOH+ 0.01 *M* KI + 1 *M* KCl, flow rate: 2 *ml*/min, scan rate: 90 mV/min, deposition potential: −1.3 V *vs.* SSE.

the second one is the detector. The potential of the first cell is set initially at −1.3 V *vs.* SSE, and the carrier solution containing very dilute lead ions, after deoxygenated, was constantly passed through it at 2 *ml*/min for a definite time to concentrate lead on the electrode. After the concentration step, the potential was scanned linearly at 90 mV/min toward the positive direction up to 0 V *vs.* SSE to strip out the deposited lead. The eluted lead ions were sent and detected in the second cell at a constant potential of −0.7 V *vs.* SSE. The detection current was recorded against the scanning potential of the first cell. Figure 15 shows the stripping coulopotentiogram of 250 *ml* of 10^{-8} *mol*/*l* Pb^{2+}. Wave A is a lead wave, and wave B seems to be a copper wave contaminated in the supporting electrolyte.

The number of coulombs consumed in detection was obtained by integrating the peak area in the stripping curve, and the amount of lead was calculated directly from Faraday's equation.

Figure 16 shows the calibration curves for a dilute sample of lead ions. The supporting electrolyte solution was contaminated with 3×10^{-9} *mol*/*l* of lead ions. In the analysis of very dilute solutions, interference from trace impurities contained in the supporting electrolyte is to some extent unavoidable.

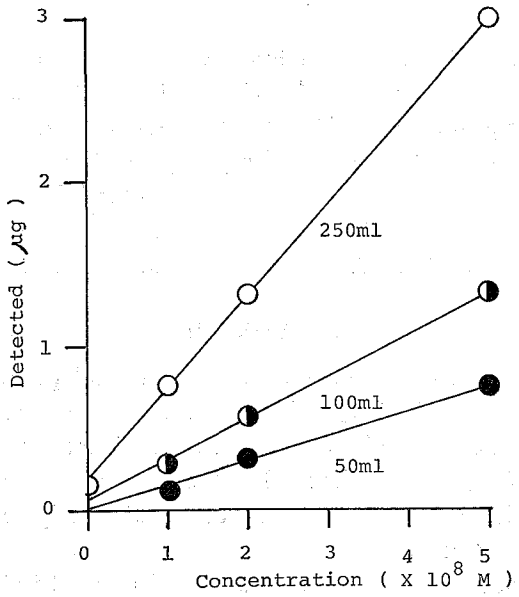

Fig. 16. Calibration curves for trace lead ions.
Carrier solution: 0.1 *M* CH_3COOH + 0.01 *M* KI + 1 *M* KCl,
flow rate: 2 *ml*/min, scan rate: 90 mV/min, depositon potential:
−1.3 V *vs.* SSE.

Half-wave Potentials and Stripping Peak Potentials of Inorganic Ions

Half-wave potentials (upward) and stripping peak potentials (downward) of various inorganic elements in several kinds of carrier solutions are summarized in Table IV. Upward and downward arrows show the usable potential ranges in the negative and positive scan, respectively.

Table IV. Half-wave potentials and stripping peak potentials.

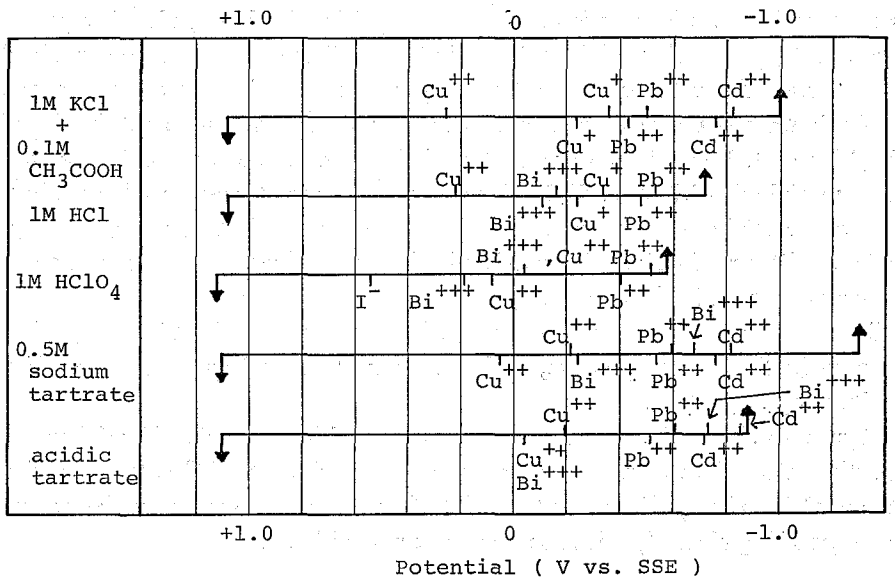

The measuring conditions were as follows; For the measurements of the half-wave potentials, the concentration was 10^{-4} *mol/l*, the flow rate was 2 *ml*/min, and the scan rate was 2.67 mV/min. For stripping peak potentials, the amounts of the sample were 5×10^{-7} *moles* each, the flow rate was 2 *ml*/min, and the scan rate was 40 mV/min.

Usable potential ranges were defined as the potential difference between the negative and the positive potentials at which the base current is ± 0.5 mA at the potential scanning rate of 2.67 mV/min and the flow rate of 2 *ml*/min.

CONCLUSION

As mentioned above, there are many methodological possibilities in analytical chemistry as well as electrochemistry. These methods not only have great advantages of absolute determinations but also offer great convenience for continuous and simultaneous analysis of trace metal ions. Furthermore, these methods have the advantage of being able to be applied to the automatic analyzer owing to the simplicity of the instrumentation.

Strictly speaking, however, the methods should be modified from the following viewpoints; 1) elimination of interference by the impurities in the supporting electrolyte, 2) elimination of interference by pre-discharging ions in the sample, 3) development of an automatic controlling system.

The authors are currently developing an automated coulopotentiographic analyzer system and will present the result elsewhere.

REFERENCES

(1) E.L. Eckfeldt, *Anal. Chem.*, **31**, 1453 (1959).
(2) T. Fujinaga, T. Nagai, C. Takagi, and S. Okazaki, *Nippon Kagaku Zasshi*, **84**, 941 (1963).

(3) T. Fujinaga, K. Izutsu, and S. Okazaki, *Rev. Polarog.*, **14**, 164 (1967).
(4) T. Fujinaga, *Pure Appl. Chem.*, **25**, 709 (1971).
(5) W.J. Blaedel and J.H. Strohl, *Anal. Chem.*, **36**, 1245 (1964).
(6) A.J. Bard, *Anal. Chem.*, **35**, 1125 (1963).
(7) G. Johanson, *Talanta*, **12**, 163 (1965).
(8) Y. Takata and G. Muto, *Bunseki Kagaku*, **14**, 453 (1965); **15**, 154 (1966).
(9) S. Okazaki, *Rev. Polarog.*, **15**, 269 (1968).
(10) S. Kihara, *J. Electroanal. Chem.*, **38**, 51 (1972).
(11) T. Fujinaga, C. Takagi, and S. Okazaki, *Kogyo Kagaku Zasshi*, **67**, 1798 (1964).
(12) T. Fujinaga, S. Okazaki, K. Izutsu, M. Koyama, and K. Tsuji, *Nippon Kagaku Zasshi*, **89**, 673 (1968).
(13) R.C. Propst, *Anal. Chem.*, **35**, 958 (1963).
(14) T. Fujinaga, S. Okazaki, and T. Yamada, *Chemistry Letters*, 863 (1972).
(15) T. Fujinaga, S. Okazaki, and T. Yamada, *ibid*, 1295 (1973).
(16) J.J. Lingane, *Anal. Chim., Acta*, **2**, 591 (1948).
(17) E.L. Eckfeldt and E.W. Shaffer, Jr., *Anal. Chem.*, **36**, 2008 (1964).